Available online at www.sciencedirect.com
SCIENCE DIRECT®
Journal of Organometallic Chemistry 690 (2005) 4027–4035
Journal of Organometallic Chemistry
www.elsevier.com/locate/jorganchem

Formation of new organometallic W/Cu/S clusters from reactions of $[\{(\eta^5\text{-}C_5Me_5)WS_3\}_3Cu_7(MeCN)_9](PF_6)_4$ with donor ligands. Crystal structures and optical limiting properties of $[(\eta^5\text{-}C_5Me_5)WS_3Cu_3(Py)_6](PF_6)_2$, $[(\eta^5\text{-}C_5Me_5)WS_3Cu_3Br(PPh_3)_3](PF_6)$, and $[(\eta^5\text{-}C_5Me_5)WS_3Cu_4(Py)Cl(dppm)_2](PF_6)_2$

Hong Yu [a,*], Wen-Hua Zhang [a], Zhi-Gang Ren [a], Jin-Xiang Chen [a], Chun-Lan Wang [a], Jian-Ping Lang [a,b,*], Hendry Izaac Elim [c], Wei Ji [c]

[a] *Key Laboratory of Organic Chemistry of Jiangsu Province, School of Chemistry and Chemical Engineering, Suzhou University, No. 1 Shizi Street, Suzhou 215006, Jiangsu, PR China*
[b] *State Key Laboratory of Structural Chemistry, Fujian Institute of Research on the Structure of Matter, Chinese Academy of Sciences, Fuzhou 350002, Fujian, PR China*
[c] *Department of Physics, National University of Singapore, 2 Science Drive 3, 117542 Singapore*

Received 3 April 2005; received in revised form 28 May 2005; accepted 2 June 2005
Available online 14 July 2005

Abstract

Treatment of a preformed cluster $\{(\eta^5\text{-}C_5Me_5)WS_3\}_3Cu_7(MeCN)_9](PF_6)_4$ (**1**) in MeCN with excess pyridine afforded a tetranuclear cationic cluster $[(\eta^5\text{-}C_5Me_5)WS_3Cu_3(Py)_6](PF_6)_2$ (**2**). On the other hand, reactions of **1** with excess PPh_3 under the presence of LiBr gave rise to the other tetranuclear cationic cubane-type cluster $[(\eta^5\text{-}C_5Me_5)WS_3Cu_3Br(PPh_3)_3](PF_6)$ (**3**) while analogous reactions of **1** with dppm and LiCl followed by addition of excess pyridine generated an intriguing pentanuclear cationic cluster $[(\eta^5\text{-}C_5Me_5)WS_3Cu_4(Py)Cl(dppm)_2](PF_6)_2$ (**4**). Compounds **2**–**4** were fully characterized by spectroscopy and X-ray crystallography. The cluster dication of **2** adopts an incomplete WS_3Cu_3 cubane-like structure while the cluster cation of **3** contains a WS_3Cu_3Br cubane-like structure. The structure of the cluster dication of **4** consists of an unique WS_3Cu_4Cl framework in which an open cubane-like WS_3Cu_3Cl fragment and a $Cu(dppm)_2$ fragment are connected by one Cu–Cl bond and two Cu–dppm–Cu bridges. The optical limiting (OL) properties of the MeCN solutions of **1**–**4** were investigated with 7-ns laser pulses at 532 nm.

Keywords: Tungsten cluster; Copper cluster; Sulfide cluster; Crystal structures; Optical limiting properties

1. Introduction

In the past decades, synthesis of Mo(W)/Cu/S clusters has attracted much interest due to their interesting chemistry [1–11], and their potential applications in biological systems [1,4,10] and electro/photonic materials [7,8f,9f,9g,11]. There are several approaches to the construction of the Mo(W)/Cu/S clusters. The first one is the "one-pot" synthesis, in which thiometallates (e.g. $[MO_{4-n}S_n]^{2-}$ (M = Mo, W; n = 1–4) and $[(\eta^5\text{-}C_5Me_5)MS_3]^-$ (M = Mo, W)) were mixed with Cu(I) salts or complexes in organic solvents to generate various Mo(W)/Cu/S clusters, which could be found in

* Corresponding authors. Tel.: +86 512 65213506; fax: +86 512 65224783.
E-mail addresses: yuhong@suda.edu.cn (H. Yu), jplang@suda.edu.cn (J.-P. Lang).

0022-328X/$ - see front matter © 2005 Elsevier B.V. All rights reserved.
doi:10.1016/j.jorganchem.2005.06.003

numerous literatures [1–9,11]. The second one is that a preformed small Mo(W)/Cu/S cluster is used to react with certain donor ligands (e.g. S^{2-}, 4,4′-bipy), yielding larger clusters or polymeric clusters [3,5c,6b,9e–9g]. The third one, which is less explored, is involved in the formation of a smaller cluster from the reaction of a preformed cluster with donor ligands (e.g. 2,2′-bipy and PPh_3) [9c,9e,12]. For example, reaction of $[NEt_4]_4[WS_4Cu_5Cl_7]$ with 2,2′-bipyridine and PPh_3 afforded $[WS_4Cu_3Cl(2,2'\text{-bipy})]_n$ and $[WS_4Cu_3(PPh_3)_3Cl]$, respectively [12a]. In the two reactions, the $[WS_4Cu_5]$ framework was turned into a smaller incomplete WS_4Cu_3 cubane-shaped core.

On the other hand, we have been interested in the preparation and third-order non-linear optical properties of Mo(W)/Cu/S clusters over the last ten years [8b,8c,8e,8f,9]. We once communicated an interesting reaction in which $[\{(\eta^5\text{-}C_5Me_5)WS_3\}_3Cu_7(MeCN)_9](PF_6)_4$ (**1**) reacted with 1,4-pyrazine (1,4-pyz) under the presence of LiCl, forming an interesting 2D polymer $\{[(\eta^5\text{-}C_5Me_5)WS_3Cu_3Cl(MeCN)(1,4\text{-pyz})](PF_6)\}_\infty$ [9e]. In this reaction, the triple incomplete cubane-like $[W_3S_9Cu_7]$ framework of **1** was turned into a smaller incomplete WS_3Cu_3 cubane-like framework. In addition, we are involved in the construction of Mo(W)/Cu/S clusters from some preformed clusters with luminescent or optical limiting properties [9g,9f]. As discussed later in this paper, the solution of compound **1** exhibited slightly better optical limiting (OL) performance than that of C_{60}. Therefore, is it possible to use **1** as a useful precursor to make other new W/Cu/S clusters with better OL properties via its reactions with other donor ligands? With the question in mind, we carried out reactions of **1** with Py, PPh_3, and dppm, and some in the presence of LiX (X = Cl, Br). Three novel smaller W/Cu/S clusters $[(\eta^5\text{-}C_5Me_5)WS_3Cu_3(Py)_6](PF_6)_2$ (**2**) $[(\eta^5\text{-}C_5Me_5)WS_3Cu_3Br(PPh_3)_3](PF_6)$ (**3**) and $[(\eta^5\text{-}C_5Me_5)WS_3Cu_4(Py)Cl(dppm)_2](PF_6)_2$ (**4**) were produced in relatively high yields. Furthermore, we have also examined the OL properties of **1**–**4** in acetonitrile with 7-ns laser pulses at 532 nm. Herein, we report their preparation and structural characterization along with their OL properties in solution.

2. Results and discussion

2.1. Synthesis and spectral characterization

As shown in Scheme 1, reaction of **1** in MeCN with excess Py formed a homogeneous solution, from which $[(\eta^5\text{-}C_5Me_5)WS_3Cu_3(Py)_6](PF_6)_2$ (**2**) was isolated as dark red plates in 65% yield. We once reported that lithium halide sometimes proved to be useful in making cluster-based supramolecular compounds [9e,9f]. For example, reactions of $[PPh_4][(\eta^5\text{-}C_5Me_5)WS_3Cu_3(CN)_3]$ with 1,4-pyrazine under the presence of LiCl yielded a supramolecular cube $[\{(\eta^5\text{-}C_5Me_5)WS_3Cu_3\}_8Cl_8(CN)_{12}Li_4]$ [9f]. In the structure of this compound, each chloride interacts weakly with three copper atoms of the $(\eta^5\text{-}C_5Me_5)WS_3Cu_3$ core, which may stabilize the resulting cluster framework. However, analogous reaction of **1** in MeCN with excess Py in the presence of LiCl (4 equiv.) gave rise to the same cluster **2** in 60% yield. When excess PPh_3 was added into the acentonitrile solution of **1**, it formed a clear red solution, from which a red product was isolated after a workup. According to its elemental analysis, X-ray fluorescence analysis and IR spectrum, we tentatively assumed its chemical formula to be $[(\eta^5\text{-}C_5Me_5)WS_3Cu_3(PPh_3)_3](PF_6)_2$. Interest-

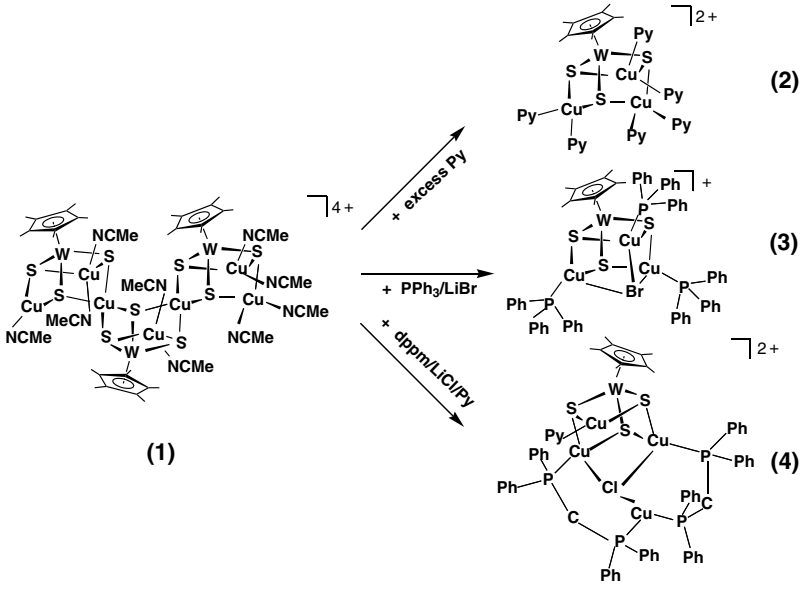

Scheme 1.

ingly, when we added 2.4 equiv. of LiBr into its red solution, a similar workup generated $[(\eta^5\text{-}C_5Me_5)WS_3Cu_3Br(PPh_3)_3](PF_6)$ (**3**) as red prisms in 68% yield. In the presence of LiCl, the analogous reaction of **1** with PPh_3 afforded a similar product to **3**. However, numerous attempts to grow its crystals of good quality failed.

On the other hand, treatment of **1** in MeCN with excess dppm also gave rise to a clear solution, from which a dark red product was isolated after a workup. However, attempts to characterize the identity of the resulting product failed according to its elemental analysis, X-ray fluorescence analysis and IR spectrum. When LiCl was introduced into its solution, a red precipitate was gradually formed. The resulting solid was insoluble in common organic solvents, which excluded the further characterization of its identity. Considering that pyridine (Py) can be used a solvent and a ligand [9g], we treated the mixture with pyridine to produce $[(\eta^5\text{-}C_5Me_5)WS_3Cu_4(Py)Cl(dppm)_2](PF_6)_2$ (**4**) as red crystals in 46% yield.

Compounds **2**–**4** are air and moisture stable in the solid state. They are slightly soluble in CH_2Cl_2, $CHCl_3$, and MeOH, but readily soluble in MeCN, DMF, and DMSO. The elemental analysis of **2**–**4** is consistent with their chemical formula. The FT-IR spectra of **2**–**4** displayed bands arising from the W–S_{br} stretching vibrations at 425/408 (**2**), 425/410 (**3**), and 417/409 (**4**) cm^{-1}, respectively. For **2**–**4**, strong peaks arising from PF_6 also appeared at 841 and 556 (or 557) cm^{-1}. The ^1H NMR spectra of **2**–**4** in CD_3CN, measured at ambient temperature, showed a single resonance of $\eta^5\text{-}C_5Me_5$ group at 2.14 (**2**), 2.18 (**3**), and 2.12 (**4**) ppm, respectively. For **4**, the methylene protons of each dppm ligand split into two broad multiplet signals. As shown in Fig. 1, the UV–Vis spectra of **1**–**2** in MeCN are characterized by one band at 406 (**1**) or 402 nm (**2**), while those of **3**–**4** in MeCN have two absorptions at 326/398 nm (**3**) or 328/398 nm (**4**). As the electronic spectrum of $[PPh_4][(\eta^5\text{-}C_5Me_5)WS_3]$ in MeCN has a strong absorption band at 381 nm [13], the bands at 406 (**1**), 402 (**2**), 398 (**3**), and 398 (**4**) nm observed in the UV–Vis spectra of **1**–**4** are red-shifted, and they are probably dominated by the S → W(VI) charge-transfer transitions of $\eta^5\text{-}(C_5Me_5)WS_3$ moiety [9c,9g]. The crystal structures of **2**–**4** were further confirmed by single-crystal X-ray analysis.

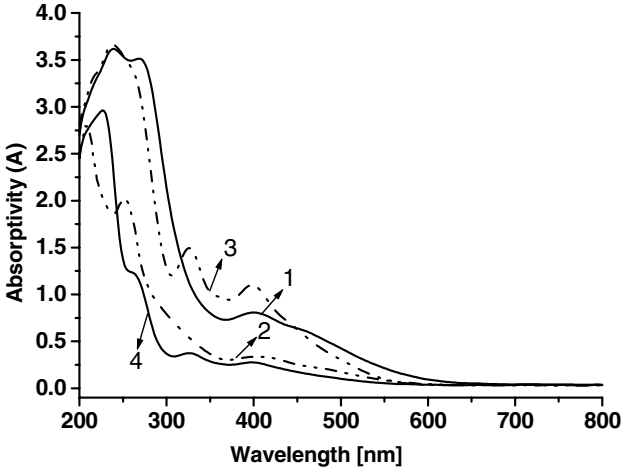

Fig. 1. Absorption spectra of **1**–**4** in MeCN with a 1-mm optical length.

2.2. Crystal structure of $[(\eta^5\text{-}C_5Me_5)WS_3Cu_3(Py)_6](PF_6)_2$ (2)

Compound **2** crystallizes in the monoclinic space group *C2/c*, and the asymmetric unit contains one discrete dication $[(\eta^5\text{-}C_5Me_5)WS_3Cu_3(Py)_6]^{2+}$, two $[PF_6]^-$ anions, and one pyridine solvated molecule. Fig. 2 shows the structure of the cluster $[(\eta^5\text{-}C_5Me_5)WS_3Cu_3(Py)_6]^{2+}$ dication of **2**, and Table 1 lists its selected bond distances and angles. The cluster dication of **2** contains an incomplete $[WS_3Cu_3]$ cubane-like structure in which a $[(\eta^5\text{-}C_5Me_5)WS_3]^-$ anion is coordinated by three $[Cu(py)_2]^+$ cations via S atoms. The oxidation states for W and Cu atoms are retained as +6, and +1, respectively. This structure is closely related to $[MOS_3Cu_3(4\text{-pic})_6][Mo_2O_7]_{0.5}$ and $[MOS_3Cu_3(4\text{-pic})_6](BF_4)$ (M = Mo, W, 4-pic = 4-picoline) [14]. The $[(\eta^5\text{-}C_5Me_5)WS_3]^-$ anion of **2** has a slightly distorted three-legged piano stool structure. The mean W–μ_3-S bond length (2.2857(14) Å), is elongated by 0.02 Å compared with that of $[PPh_4][(\eta^5\text{-}C_5Me_5)WS_3]$ [13] as a consequence of coordination of S atoms to Cu atoms. Each copper atom in **2** exhibits a distorted tetrahedral geometry, coordinated by two μ_3-S and two N(Py) atoms. The mean W···Cu contact of 2.6933(7) Å of **2** is close to that

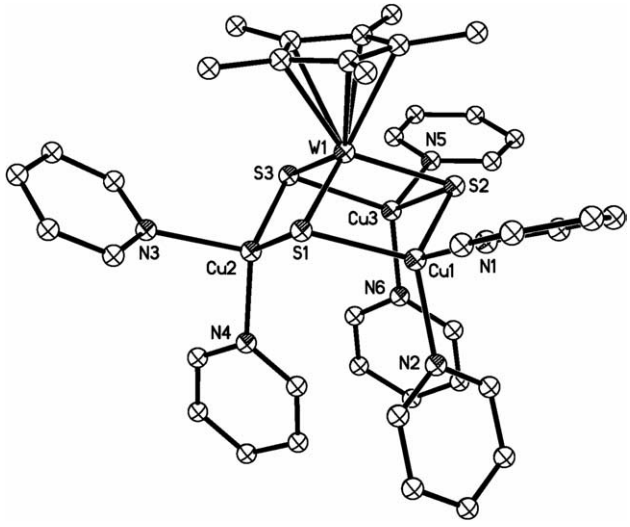

Fig. 2. The perspective view of the cluster dication of **2**. The thermal ellipsoids are drawn at the 50% probability level and the hydrogen atoms are omitted for clarity.

Table 1
Selected bond lengths (Å) and angles (°) of **2**

W(1)···Cu(1)	2.6970(7)	W(1)···Cu(2)	2.6965(7)
W(1)···Cu(3)	2.6865(7)	W(1)–S(1)	2.2883(12)
W(1)–S(2)	2.2841(12)	W(1)–S(3)	2.2846(13)
Cu(1)–S(1)	2.2387(14)	Cu(1)–S(2)	2.2450(14)
Cu(2)–S(1)	2.2555(14)	Cu(2)–S(3)	2.2502(14)
Cu(3)–S(2)	2.2328(14)	Cu(3)–S(3)	2.2423(15)
Cu(1)–N(1)	2.141(4)	Cu(1)–N(2)	2.024(4)
Cu(2)–N(3)	2.111(4)	Cu(2)–N(4)	2.018(4)
Cu(3)–N(5)	2.108(4)	Cu(3)–N(6)	2.041(4)
Cu(1)···W(1)···Cu(2)	82.02(2)	Cu(1)···W(1)···Cu(3)	81.74(2)
Cu(2)···W(1)···Cu(3)	79.18(2)	S(1)–W(1)–S(2)	105.35(4)
S(1)–W(1)–S(3)	105.92(5)	S(2)–W(1)–S(3)	105.44(5)
S(1)–Cu(1)–S(2)	108.38(5)	S(1)–Cu(1)–N(1)	110.54(13)
S(2)–Cu(1)–N(1)	104.56(13)	S(1)–Cu(1)–N(2)	115.53(13)
S(2)–Cu(1)–N(2)	121.27(13)	N(1)–Cu(1)–N(2)	94.75(17)
S(1)–Cu(2)–S(3)	108.22(5)	S(1)–Cu(2)–N(3)	101.67(12)
S(3)–Cu(2)–N(3)	108.30(12)	S(1)–Cu(2)–N(4)	122.87(12)
S(3)–Cu(2)–N(4)	112.22(13)	N(3)–Cu(2)–N(4)	101.99(17)
S(2)–Cu(3)–S(3)	108.64(5)	S(2)–Cu(3)–N(5)	106.69(14)
S(3)–Cu(3)–N(5)	109.39(14)	S(2)–Cu(3)–N(6)	121.09(13)
S(3)–Cu(3)–N(6)	115.81(14)	N(5)–Cu(3)–N(6)	93.22(17)
W(1)–S(1)–Cu(1)	73.12(4)	W(1)–S(1)–Cu(2)	72.80(4)
Cu(1)–S(1)–Cu(2)	103.90(5)	W(1)–S(2)–Cu(1)	73.09(4)
W(1)–S(2)–Cu(3)	72.98(4)	Cu(1)–S(2)–Cu(3)	103.76(6)
W(1)–S(3)–Cu(2)	72.97(4)	W(1)–S(3)–Cu(3)	72.80(4)
Cu(2)–S(3)–Cu(3)	99.56(5)		

found in $[WOS_3Cu_3(4\text{-pic})_6](BF_4)$ (2.7037(10) Å) [14], but shorter than those reported in $[WS_4Cu_4(dppm)_4](PF_6)_2$ (av. 2.760(2) Å) [8c] and $[(\eta^5\text{-}C_5Me_5)WS_3Cu]_4$ (av. 2.749(3) Å) [9d]. The mean Cu–μ_3-S bond lengths of 2.2441(14) Å is shorter than those found in $[(\eta^5\text{-}C_5Me_5)WS_3Cu]_4$ (2.290(7) Å), $[WOS_3Cu_3(4\text{-pic})_6](BF_4)$ (2.295(2) Å), and $[WS_4Cu_4(dppm)_4](PF_6)_2$ (av. 2.351(4) Å). The mean Cu–N length (2.104(4) Å) is longer than those observed in $[WOS_3Cu_3(4\text{-pic})_6](BF_4)$ (2.064(7) Å) and $[Cu(Py)_4]ClO_4$ (2.046(3) Å) [15].

2.3. Crystal structure of $[(\eta^5\text{-}C_5Me_5)WS_3Cu_3Br(PPh_3)_3](PF_6)$ (3)

Compound $\mathbf{3}\cdot 0.5C_6H_6$ crystallizes in the monoclinic space group $P2_1/a$, and the asymmetric unit contains one independent cation $[(\eta^5\text{-}C_5Me_5)WS_3Cu_3Br(PPh_3)_3]^+$, one $[PF_6]^-$ anion, and one half of a benzene solvated molecule. Fig. 3 shows the perspective view of the cluster cation of **3** and Table 2 lists the selected bond distances and angles of the cluster cation of **3**. The cluster cation of **3** consists of a strongly distorted WS_3Cu_3Br cubane structure in which Br(1) fills into the void of the incomplete $[WS_3Cu_3]$ cube with one short and two long Cu–Br distances (Cu(3)–Br(1) = 2.6374(9) Å, Cu(1)–Br(1) = 2.7355(9) Å, Cu(2)–Br(1) = 2.7693(10) Å). The resulting cube is closely related to those found in neutral Mo(W)/Cu/S clusters, e.g. $[MOS_3Cu_3(PPh_3)_3X]$ (M = Mo, W; X = Cl [16]; M = Mo, E = O, X = Br [1b]). The three Cu atoms in the cube of **3** are not equivalent, and their coordination variability ranges from a strongly distorted tetrahedron (Cu(3)) to a nearly trigonal planar coordination (Cu(1) and Cu(2)) with a long Cu–Br(1) interaction. Because of the different coordination geometries of the copper atoms, the W···Cu separations are different: W(1)···Cu(1) = 2.702(1) Å, W(1)···Cu(2) = 2.7087(9) Å, and W(1)···Cu(3) = 2.7414(8) Å, which correlates with the number of bonding interactions at Cu centers.

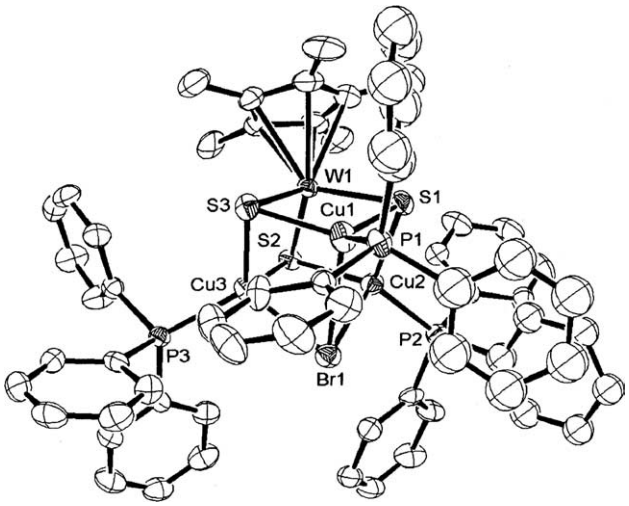

Fig. 3. The perspective view of the cluster cation of **3**. The thermal ellipsoids are drawn at the 50% probability level and the hydrogen atoms are omitted for clarity.

Table 2
Selected bond lengths (Å) and angles (°) of **3**

W(1)···Cu(1)	2.702(1)	W(1)···Cu(2)	2.7087(9)
W(1)···Cu(3)	2.7414(8)	W(1)–S(1)	2.286(2)
W(1)–S(2)	2.274(1)	W(1)–S(3)	2.270(2)
Br(1)–Cu(1)	2.770(1)	Br(1)–Cu(2)	2.733(1)
Br(1)–Cu(3)	2.636(2)	Cu(1)–S(1)	2.255(2)
Cu(1)–S(3)	2.263(3)	Cu(2)–S(2)	2.263(2)
Cu(2)–S(1)	2.269(2)	Cu(3)–S(2)	2.277(2)
Cu(3)–S(3)	2.298(2)	Cu(1)–P(1)	2.230(3)
Cu(2)–P(2)	2.221(2)	Cu(3)–P(3)	2.230(2)
Cu(2)···W(1)···Cu(1)	68.94(3)	Cu(3)···W(1)···Cu(1)	69.90(3)
Cu(3)···W(1)···Cu(2)	67.36(3)	S(2)–W(1)–S(1)	105.10(7)
S(3)–W(1)–S(1)	105.59(8)	S(3)–W(1)–S(2)	105.54(6)
Br(1)–Cu(1)–S(1)	100.73(5)	Br(1)–Cu(1)–S(3)	96.81(6)
Br(1)–Cu(1)–P(1)	103.72(7)	S(3)–Cu(1)–S(1)	106.86(9)
P(1)–Cu(1)–S(1)	119.99(9)	P(1)–Cu(1)–S(3)	123.16(9)
Br(1)–Cu(2)–S(1)	101.44(6)	Br(1)–Cu(2)–S(2)	100.26(6)
Br(1)–Cu(2)–P(2)	106.13(6)	S(2)–Cu(2)–S(1)	106.04(8)
P(2)–Cu(2)–S(1)	118.16(8)	P(2)–Cu(2)–S(2)	121.39(8)
Br(1)–Cu(3)–S(2)	102.82(7)	Br(1)–Cu(3)–S(3)	99.75(7)
Br(1)–Cu(3)–P(3)	113.24(7)	S(3)–Cu(3)–S(2)	104.54(7)
P(3)–Cu(3)–S(2)	116.33(8)	P(3)–Cu(3)–S(3)	117.89(8)
Cu(1)–S(1)–Cu(2)	85.22(7)	Cu(1)–S(3)–Cu(3)	86.27(8)
Cu(2)–S(2)–Cu(3)	83.47(8)	Cu(2)–Br(1)–Cu(1)	67.62(3)
Cu(3)–Br(1)–Cu(1)	70.41(4)	Cu(3)–Br(1)–Cu(2)	68.48(4)
W(1)–S(1)–Cu(1)	73.04(7)	W(1)–S(1)–Cu(2)	72.98(6)
W(1)–S(2)–Cu(2)	73.30(6)	W(1)–S(2)–Cu(3)	74.07(5)
W(1)–S(3)–Cu(1)	73.17(7)	W(1)–S(3)–Cu(3)	73.76(6)

The short W(1)···Cu(1) and W(1)···Cu(2) contacts are in-between those observed in clusters containing trigonally-coordinated Cu such as $[PPh_4][\{(\eta^5\text{-}C_5Me_5)\text{-}WS_3\text{-}Cu_2\}_2S_2]$ (2.665(2)–2.683(3) Å) [9b] and $[WOS_3Cu_3(PPh_3)_3Cl]$ (2.721(2)–2.730(2) Å) [16]. The long W(1)···Cu(3) separation is longer than that of **2** described above. The various Cu–μ_3-S bond lengths also show the different coordination modes of the three Cu atoms in **3**. For a trigonally-coordinated Cu, the average Cu–μ_3-S bond length (2.254(2) Å) is slightly longer than those reported in other trigonally-coordinated Cu clusters such as $[PPh_4]_2[(\eta^5\text{-}C_5Me_5)WS_3Cu_3Br_3]_2$ (2.234(2) Å) [9a] and $[PPh_4][\{(\eta^5\text{-}C_5Me_5)WS_3Cu_2\}_2S_2]$ (2.230(6) Å) [9b]. For a tetrahedrally-coordinated Cu, the mean Cu–μ_3-S bond length (2.286(2) Å) is somewhat longer than that of **2**. The mean Cu–μ_3-Br length of 2.741(1) Å is ca. 0.1 Å longer than those observed in $[MoOS_3\text{-}Cu_3(PPh_3)_3Br]$ (av. Cu–μ_3-Br = 2.635(1) Å) [1b]. The mean W–μ_3-S distance of **3** (2.277(2) Å) is slightly shorter than that of **2**.

2.4. Crystal structure of $[(\eta^5\text{-}C_5Me_5)WS_3Cu_4(Py)\text{-}Cl(dppm)_2](PF_6)_2$ (4)

Compound **4** crystallizes in the orthorhombic space group *Pbca*, and the asymmetric unit contains one discrete $[(\eta^5\text{-}C_5Me_5)WS_3Cu_4(Py)Cl(dppm)_2]^{2+}$ dication, two $[PF_6]^-$ anions, and two MeCN solvated molecules. Fig. 4 shows only the structure of the cluster dication of **4** and Table 3 lists the important bond distances and angles of the cluster dication of **4**. The cluster dication of **4** contains a WS_3Cu_4Cl core structure in which a

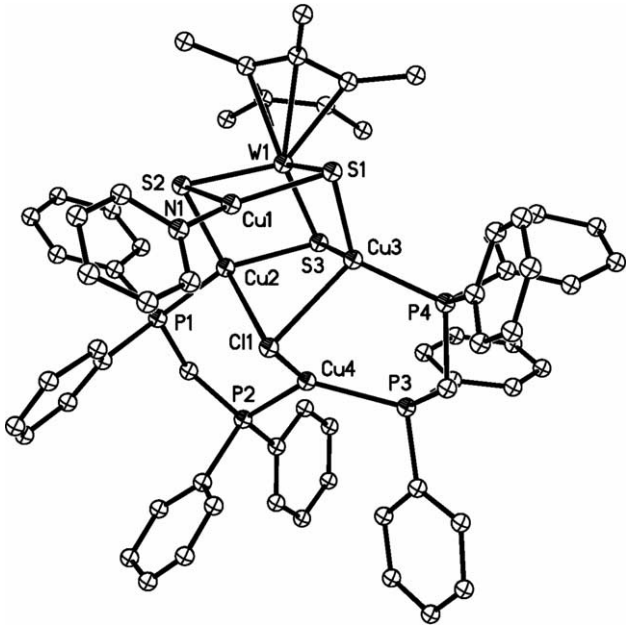

Fig. 4. The perspective view of the cluster dication of **4**. The thermal ellipsoids are drawn at the 50% probability level and the hydrogen atoms are omitted for clarity.

Table 3
Selected bond lengths (Å) and angles (°) of **4**

W(1)···Cu(1)	2.631(2)	W(1)···Cu(2)	2.687(2)
W(1)···Cu(3)	2.700(2)	W(1)–S(1)	2.285(4)
W(1)–S(2)	2.277(4)	W(1)–S(3)	2.296(4)
Cu(1)–S(1)	2.215(5)	Cu(1)–S(2)	2.216(4)
Cu(2)–S(2)	2.242(4)	Cu(2)–S(3)	2.243(4)
Cu(3)–S(1)	2.252(4)	Cu(3)–S(3)	2.259(4)
Cu(2)–Cl(1)	2.871(3)	Cu(3)–Cl(1)	2.673(3)
Cu(4)–Cl(1)	2.393(3)	Cu(2)–P(1)	2.206(4)
Cu(3)–P(4)	2.225(4)	Cu(4)–P(2)	2.266(4)
Cu(4)–P(3)	2.282(4)	Cu(1)–N(1)	1.913(12)
Cu(1)···W(1)···Cu(2)	72.46(6)	Cu(1)···W(1)···Cu(3)	72.91(8)
Cu(2)···W(1)···Cu(3)	71.36(6)	S(1)–W(1)–S(2)	105.75(15)
S(1)–W(1)–S(3)	105.27(13)	S(2)–W(1)–S(3)	105.11(13)
S(1)–Cu(1)–S(2)	110.33(16)	S(1)–Cu(1)–N(1)	130.8(4)
S(2)–Cu(1)–N(1)	117.6(4)	Cl(1)–Cu(2)–S(2)	106.22(14)
Cl(1)–Cu(2)–S(3)	92.67(12)	Cl(1)–Cu(2)–P(1)	106.10(13)
S(2)–Cu(2)–S(3)	108.10(16)	S(2)–Cu(2)–P(1)	109.57(16)
S(3)–Cu(2)–P(1)	130.58(16)	Cl(1)–Cu(3)–S(1)	107.13(14)
Cl(1)–Cu(3)–S(3)	97.73(14)	Cl(1)–Cu(3)–P(4)	103.46(14)
S(1)–Cu(3)–S(3)	107.60(15)	S(1)–Cu(3)–P(4)	112.11(16)
S(3)–Cu(3)–P(4)	126.22(15)	Cl(1)–Cu(4)–P(2)	119.54(14)
Cl(1)–Cu(4)–P(3)	109.45(14)	P(2)–Cu(4)–P(3)	124.68(15)
Cu(2)–Cl(1)–Cu(3)	68.92(8)	Cu(2)–Cl(1)–Cu(4)	71.4(1)
Cu(3)–Cl(1)–Cu(4)	78.54(11)	W(1)–S(1)–Cu(1)	71.52(13)
W(1)–S(1)–Cu(3)	73.04(13)	Cu(1)–S(1)–Cu(3)	89.71(16)
W(1)–S(2)–Cu(1)	71.66(12)	W(1)–S(2)–Cu(2)	72.96(11)
Cu(1)–S(2)–Cu(2)	90.28(14)	W(1)–S(3)–Cu(2)	72.57(11)
W(1)–S(3)–Cu(3)	72.70(12)	Cu(2)–S(3)–Cu(3)	88.49(15)

$[(\eta^5\text{-}C_5Me_5)WS_3Cu_3(Py)Cl]^+$ fragment and a $[Cu(dppm)_2]^+$ fragment are connected by the Cu(4)–Cl(1) bond and a pair of Cu–dppm–Cu bridges. To our knowledge, such a cluster framework has no counterpart in the thiometallates. The main structural feature of the $[(\eta^5\text{-}C_5Me_5)WS_3Cu_3(Py)Cl]^+$ fragment in **4** consists of a distorted WS_3Cu_3Cl cube where the Cu(1)–Cl(1) bond is broken, which resembles those of $[(\eta^5\text{-}C_5Me_5)WS_3Cu_3Br_2(PPh_3)_2]$ [9c] and $[NEt_4]_3[WOS_3\text{-}Cu_3Br_4]\cdot 2H_2O$ [17]. Cu(1) assumes a trigonal-planar geometry, coordinated by one N(Py) and two μ_3-S atoms. On the other hand, Cu(2) and Cu(3) atoms adopt a distorted tetrahedral geometry, coordinated by one μ_3-Cl, one P(dppm) and two μ_3-S atoms. Therefore the different coordination modes of the three Cu atoms results in the difference of the W(1)···Cu contacts within the $[(\eta^5\text{-}C_5Me_5)WS_3Cu_3(Py)Cl]^+$ fragment. The trigonally-coordinated W(1)···Cu(1) contact (2.631(2) Å) is shorter than those of the corresponding ones of **3**. However, the mean W···Cu contact for four-coordinated Cu, 2.694(2) Å, is close to that of **2**, but shorter than that of the corresponding ones of **3**. The mean Cu–μ_3-S distances for Cu atoms with two different coordination modes are shorter than those of the corresponding ones of **3**. The mean Cu–N(Py) length of 1.913(12) Å of **4** is shorter than observed in clusters containing trigonally-coordinated Cu such as $[Cu(2\text{-}MePy)_3]ClO_4$ (1.99(3) Å) [18]. As the sum of the bond angles around Cu(4) is 353.7°, the coordination geometry of Cu(4) atom in a

$[Cu(dppm)_2]^+$ fragment may be considered to be a "compressed" trigonal pyramidal, coordinated by a μ_3-Cl and two P(dppm) atoms. The Cu(2)–μ_3-Cl(1) and Cu(3)–μ_3-Cl(1) bond lengths, 2.871(3) Å and 2.673(3) Å, are significantly longer than that of Cu(4)–μ_3-Cl(1) bond (2.393(3) Å). The three Cu–μ_3-Cl(1) lengths are comparable to those observed in $[WOS_3Cu_3(PPh_3)_3Cl]$ (2.457(5)–2.744(5) Å) [16]. The mean Cu-P length of **4** (2.245(4) Å) is close to those found in $[(\eta^5\text{-}C_5Me_5)WS_3Cu_3(PPh_3)_2Br_2]$ (2.247(4) Å) and $[PPh_4][(\eta^5\text{-}C_5Me_5)WS_3Cu_3Br_3(dppm)]$ (2.270(5) Å) [9c]. The mean W–μ_3-S distance and S–W–S angles of **4** are normal compared to those of the corresponding ones of **2** and **3**.

2.5. Optical limiting properties of 1–4

As shown in Fig. 1, compounds **1**–**4** have little absorption at 532 nm, which promises low intensity loss and little temperature change by photon absorption, when the laser pulse propagates in these materials. The fluence-dependent transmission measurements of **1**–**4** are depicted in Fig. 5. For **1** and **2**, the light energy transmitted starts to deviate from normal linear behavior as soon as the input light fluence reaches about 1.0 J/cm^2, and the material becomes increasingly less transparent as the light fluence rises. We define the limiting threshold as the incident fluence, at which the sample transmittance falls to 50% of the corresponding linear transmittance. The limiting threshold of compound **1** and **2** are 10 and 9.6 J/cm^2, respectively. Unfortunately, no OL effect manifests itself in compounds **3** and **4**. Even though the concentration of C_{60} (9.0×10^{-4} M) is higher than those of **1** (2.6×10^{-4} M) and 2 (3.0×10^{-4} M), the OL performance of **1** and **2** is somewhat better than that of C_{60} measured under identical conditions. Although the concentrations of **1** and **2** in solution are limited because of their poor solubility, better OL effects for them would be anticipated if higher concentrations are attained.

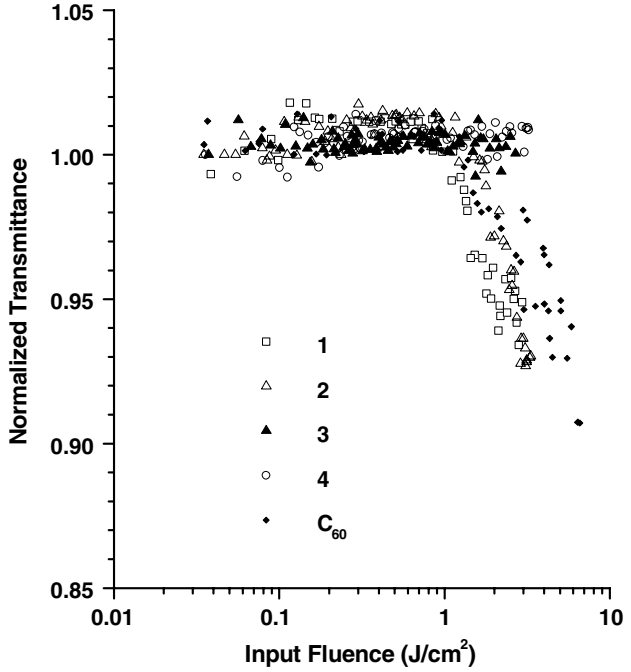

Fig. 5. Optical limiting responses to 7-ns, 532 nm laser pulses, of **1**–**4** in MeCN and C_{60} in toluene. Solutions with 92% transmittance at 532 nm correspond to 2.60×10^{-4} M (**1**), 3.00×10^{-4} M (**2**), 2.10×10^{-4} M (**3**), 1.51×10^{-4} M (**4**), and 9.00×10^{-4} M (C_{60}), respectively.

3. Conclusions

We demonstrated the successful isolation of three new W/Cu/S clusters **2**–**4** from the reactions of **1** with Py, PPh_3 and dppm in the presence or absence of LiX (X = Cl, Br). This method may be a useful route to the construction of new W/Cu/S clusters. X-ray analysis revealed that compounds **2** and **3** show an incomplete WS_3Cu_3 cubane-like structure and a WS_3Cu_3Br cubane-like structure, respectively. Compound **4** contains a half-open cubane-like WS_3Cu_3Cl fragment and a $[Cu(dppm)_2]^+$ fragment, forming a WS_3Cu_4Cl structure, which is not observed in the chemistry of the corresponding tetrathiometallates. Compounds **2**–**4** may be viewed as a set of WS_3Cu_3-based clusters. We assumed that, in all three cases, the triply-fused incomplete cubane-like framework of **1** may be converted into a smaller incomplete cubane-like WS_3Cu_3 species in solution. The different donor ligands are further coordinated to three Cu atoms of this species to yield **2**–**4**. Although the OL properties of the resulting products in this paper are not impressive, it is still worthwhile to make efforts to screen more clusters formed from the reactions of **1** with other donor ligands. Studies on this respect are currently under way in our laboratory.

4. Experimental

4.1. General

All manipulations were carried out under argon using standard Schlenk-techniques. $[\{(\eta^5\text{-}C_5Me_5)WS_3\}_3Cu_7(MeCN)_9](PF_6)_4$ (**1**) was prepared as reported previously [9e]. Other chemicals were obtained from commercial sources and used as received. All solvents were predried over activated molecular sieves and refluxed over the appropriate drying agents under argon. The IR spectra were recorded on a Nicolet MagNa-IR500 FT-IR spectrometer (4000–400 cm^{-1}). ^{1}H NMR spectra were recorded at ambient temperature on a Varian UNITYplus-400 spectrometer. UV–Vis spectra were measured on a Hitachi UV-3410 spectrophotometer.

The elemental analyses for C, H, and N were performed on a Carlo-Erba CHNO-S microanalyzer.

4.2. Synthesis

4.2.1. Preparation of $[(\eta^5\text{-}C_5Me_5)WS_3Cu_3(Py)_6](PF_6)_2$ (2)

Compound **1** (0.126 g, 0.05 mmol) was dissolved in 10 mL of pyridine. The resulting mixture was stirred at room temperature for 1 h to give a dark-red homogeneous solution. Diethyl ether (5 mL) was carefully layered onto the solution to form dark-red plates of $[(\eta^5\text{-}C_5Me_5)WS_3Cu_3(Py)_6](PF_6)_2 \cdot Py$ (**2** · Py) which were isolated by filtration, washed with Et_2O, and dried in vacuo. Yield: 0.089 g (65% based on W). Anal. Calc. for $C_{40}H_{45}Cu_3F_{12}N_6P_2S_3W$: C, 35,05; H, 3.32; N, 6.13. Found: C, 35.37; H, 3.36; N, 6.42%. IR (KBr disk): 1485 (m), 1447 (s), 1096 (m), 841 (vs), 756 (m), 702 (s), 556 (s), 425 (w), 408 (w). UV–Vis (MeCN) (λ_{max}/nm (ϵ/$M^{-1}cm^{-1}$)): 402 (2700) nm. ^{1}H NMR (CD_3CN, 400 MHz, 25 °C): δ 7.37–8.54 (m, 35H, py), 2.14 (s, 15H, η^5-C_5Me_5).

4.2.2. Preparation of $[(\eta^5\text{-}C_5Me_5)WS_3Cu_3Br(PPh_3)_3](PF_6)$ (3)

To a red solution of **1** (0.126 g, 0.05 mmol) in MeCN (10 mL) was added PPh_3 (0.085 g, 0.325 mmol). After stirring for 5 min, LiBr (0.01 g, 0.12 mmol) was added into the resulting clear red solution. The mixture was further stirred at room temperature for 1 h and then filtered. A mixed solvent containing benzene (2 mL) and diethyl ether (10 mL) was carefully layered onto the filtrate to form red needles of $[(\eta^5\text{-}C_5Me_5)WS_3Cu_3Br(PPh_3)_3](PF_6) \cdot 0.5C_6H_6$ (**3** · $0.5C_6H_6$), which were isolated by filtration, washed with Et_2O, and dried in vacuo. Yield: 0.11 g (68% based on W). Anal. Calc. for $C_{64}H_{60}Cu_3BrF_6P_4S_3W$: C, 47.52; H, 3.75. Found: C, 47.86; H, 3.83%. IR (KBr disk): 1482 (s), 1436 (s), 1378 (m), 1185 (w), 1097 (s), 1027 (m), 995 (m), 841 (s), 746 (s), 695 (s), 556 (m), 521 (s), 507 (m), 425 (w), 410 (m) cm^{-1}. UV–Vis (MeCN) (λ_{max}/nm (ϵ/$M^{-1}cm^{-1}$)): 398 (1300), 328 (1800). ^{1}H NMR (CD_3CN, 400 MHz, 25 °C): δ 7.36–7.80 (m, 45H, PPh_3), 2.18 (s, 15H, η^5-C_5Me_5).

4.2.3. Preparation of $[(\eta^5\text{-}C_5Me_5)WS_3Cu_4(Py)Cl(dppm)_2](PF_6)_2$ (4)

A solution of **1** (0.126 g, 0.05 mmol) in MeCN (10 mL) was treated with dppm (0.125 g, 0.325 mmol). After stirring for 5 min, LiCl (0.005 g, 0.12 mmol) was added into the resulting clear solution. The mixture was stirred for 30 min and a large amount of red precipitate was gradually developed. Pyridine (1 mL) was dropwise added into the mixture, which was further stirred for 30 min and then filtered. A similar work-up to that used in the isolation of **3** afforded dark-red prisms of $[(\eta^5\text{-}C_5Me_5)WS_3Cu_4(Py)Cl(dppm)_2](PF_6)_2 \cdot 2MeCN$ (**4** · 2MeCN). Yield: 0.042 g (46% based on W). Anal. Calc. for $C_{65}H_{64}ClCu_4F_{12}NP_6S_3W$: C, 42.37; H, 3,51; N, 0.76. Found: C, 42.52; H, 3.56; N, 0.84%. IR (KBr disk): 1481 (w), 1435 (m), 1381 (m), 1103 (w), 1026 (w), 841 (vs), 775 (w), 744 (m), 698 (s), 557 (m), 509 (m), 417 (w), 409 (w) cm^{-1}. UV–Vis (MeCN) (λ_{max}/nm (ϵ/$M^{-1}cm^{-1}$)): 398 (7300), 326 (9900). ^{1}H NMR (CD_3CN, 400 MHz, 25 °C): δ 7.65–8.47 (m, 5H, py), 6.98–7.54 (m, 40H, PPh_2), 3.47 (m, 2H, CH_2), 3.23 (m, 2H, CH_2), 2.12 (s, 15H, η^5-C_5Me_5).

4.2.4. X-ray diffraction crystallography

All measurements were made on a Rigaku Mercury CCD X-ray diffractometer (3 kV, sealed tube) at −80 °C by using graphite monochromated Mo Kα (λ = 0.71070 Å). A dark-red plate of **2** · Py with dimensions $0.25 \times 0.20 \times 0.05$ mm^3, a red prism of **3** · $0.5C_6H_6$ with dimensions $0.25 \times 0.20 \times 0.10$ mm^3, and a red plate of **4** · 2MeCN with dimensions $0.20 \times 0.15 \times 0.05$ mm^3, were mounted at the top of a glass fiber. Diffraction data were collected at ω mode with a detector distance of 35 mm (**2** · Py and **3** · $0.5C_6H_6$) or 55 mm (**4** · 2MeCN) to the crystal. Indexing was performed from 6 images each of which was exposed for 10 s (**2** · Py) or 20 s (**3** · $0.5C_6H_6$ and **4** · 2MeCN). A total of 720 (**2** · Py and **3** · $0.5C_6H_6$) or 1080 (**4** · 2MeCN) oscillation images were collected in the range $4.4° < 2\theta < 62.0°$ for **2** · **Py**, $4.0° < 2\theta < 62.0°$ for **3** · $0.5C_6H_6$, and $2.8° < 2\theta < 61.0°$ for **4** · 2MeCN. The collected data were reduced by using the program CrystalClear (Rigaku and MSC, Ver. 1.3, 2001), and an empirical absorption correction was applied which resulted in transmission factors ranging from 0.419 to 0.838 for **2** · Py, from 0.394 to 0.699 for **3** · $0.5C_6H_6$, and from 0.564 to 0.862 for **4** · 2MeCN. The reflection data were also corrected for Lorentz and polarization effects.

The structures of **2** · Py, **3** · $0.5C_6H_6$ and **4** · 2MeCN were solved by direct methods [19], and expanded using Fourier techniques [20]. For **2** · Py, all non-hydrogen atoms were refined anisotropically. For **3** · $0.5C_6H_6$, three phenyl groups showed sign of disorder. Two atoms (C(12) and C(13)) of the phenyl group C(11)–C(16) were modeled over two sites each with 50% occupancy. The second phenyl group C(23)–C(28) was found to be disordered over two orientations, and C(24)/C(24a), C(25)/C(25a), C(27)/C(27a) and C(28)/C(28a) were refined with occupancy factor of 0.5/0.5. The third phenyl group C(41)–C(46) were split into two orientations and C(41)/C(41a), C(42)/C(42a), C(43)/C(43a), C(44)/C(44a), C(45)/C(45a) and C(46)/C(46a) were refined as rigid groups with occupancy factors of 0.55/0.45. The non-hydrogen atoms except the C atoms of the three phenyl groups were refined anisotropically. In the case of **4** · 2MeCN, the relatively high thermal parameters of the atoms of the pyridyl group showed sign of disorder.

Table 4
Summary of crystal data for the structures of **2** · Py, **3** · 0.5C_6H_6 and **4** · 2MeCN

	2 · Py	**3** · 0.5C_6H_6	**4** · 2MeCN
Formula	$C_{45}H_{50}Cu_3F_{12}N_7P_2S_3W$	$C_{67}H_{63}BrCu_3F_6P_4S_3W$	$C_{69}H_{70}ClCu_4F_{12}N_3P_6S_3W$
F_w	1449.56	1656.69	1924.82
Crystal system	Monoclinic	Monoclinic	Orthorhombic
Space group	*C2/c*	P_1/a	*Pbca*
a (Å)	42.719(6)	17.944(2)	16.294(9)
b (Å)	15.872(2)	20.723(2)	25.077(13)
c (Å)	16.150(2)	19.211(3)	36.67(2)
β (°)	97.848(3)	113.534(3)	
V (Å^3)	10848(2)	6549.4(14)	14984(14)
Z	8	4	8
D_c (g cm^{-3})	1.775	1.680	1.706
μ (mm^{-1})	3.529	3.576	2.968
Reflections collected	64252	77955	150981
Unique reflections	15389 (R_{int} = 0.061)	18685 (R_{int} = 0.057)	22272 (R_{int} = 0.095)
Reflections ($I > 3.00\sigma(I)$)	9033	11374	7666
Parameters	708	735	861
R[a]	0.034	0.054	0.060
R_w[b]	0.038	0.065	0.073
GOF[c]	1.021	1.008	1.163
Largest residual peaks and hole/e Å^{-3}	0.90 and –0.98	1.59 and –1.01	1.73 and –1.50

[a] $R = \sum||F_o| - |F_c||/\sum|F_o|$.
[b] $R_w = \{w\sum(|F_o| - |F_c|)^2/\sum w\ F_o|^2\}^{1/2}$.
[c] GOF = $\{\sum w(|F_o| - |F_c|)^2/(MN)\}^{1/2}$, where *M* is the number of reflections and *N* is the number of parameters.

However, attempts to refine this disorder failed. All non-H atoms except those of the two $[PF_6]^-$ anions and two MeCN molecules were refined anisotropically. In the three cases, hydrogen atoms except those of the three disordered phenyl groups of **3** · 0.5C_6H_6 were placed on the idealized positions and included in the final structure-factor refinements. For **3** · 0.5C_6H_6, the largest residual electron density (1.59 e/Å^3) in the final Fourier map is close to W(1) atom (1.1 Å). For **4** · 2MeCN, the largest residual electron density (1.73 e/Å^3) in the final Fourier map is close to W(1) atom (1.25 Å). Neutral atom scattering factors were taken from Cromer and Waber [21]. Anomalous dispersion effects were included in F_{calc} [22]. All calculations were performed on a Dell workstation using the CrystalStructure crystallographic software package (Rigaku and MSC, Ver. 3.0, 2002). A summary of the key crystallographic information for **2** · Py, **3** · 0.5C_6H_6 and **4** · 2MeCN is given in Table 4.

4.2.5. Optical limiting measurements

Samples **1**–**4** were respectively dissolved in MeCN. Their solutions with concentrations of 2.60×10^{-4} M (**1**), 3.00×10^{-4} M (**2**), 2.10×10^{-4} M (**3**), and 1.51×10^{-4} M (**4**) were contained in a 1-mm-thick quartz cuvette. Optical limiting experiments were performed with a Q-switched, frequency-doubled Nd:YAG laser (λ = 532 nm) with linearly polarized 7-ns pulses. The interval between the laser pulses was set at 10 s so that every pulse of light was assured to meet fresh molecules in the sample to eliminate the influence of any photo-degradation. The optical limiting phenomenon was demonstrated by measuring fluence-dependent transmission. The laser pulses were focused on to the sample by using a focusing mirror of 25-cm focal length. The spot radius of the laser pulses at the cuvette was measured to be of 35 ± 5 μm (half width of $1/e^2$ maximum in irradiance). Both incident and transmitted laser pulses were monitored simultaneously by using a calibrated beam splitter and two energy detectors (from Laser Precision, Rjp-735 energy probes). The detectors were linked to a computer by an IEEE interface. The linear (low-intensity) transmittance of all the samples was adjusted to 92%. Fullerene (C_{60}) dissolved in toluene (9.00×10^{-4} M) was used as a standard sample since its optical limiting performance had been well-documented [23].

Acknowledgements

This work was supported by the National Natural Science Foundation of China (No. 20271036), the NSF of Jiangsu Province (No. BK2004205), the Key Laboratory of Structural Chemistry of FJISM (No. 030066), and the Scientific Research Foundation for the Returned Overseas Chinese Scholars, State Education Ministry of China. The authors highly appreciated the helpful comments and suggestions of the editor and the reviewers.

Appendix A. Supplementary data

Crystallographic data for the structural analyses have been deposited with Cambridge Crystallographic Data

Centre, CCDC Nos. 262861 (**2** · Py), 262862 (**3** · $0.5C_6H_6$) and 262863 (**4** · 2MeCN). Copies of this information may be obtained free of charge from the Director, CCDC, 12 Union Road, Cambridge CB2 1E2, UK (fax: +44 1223 336033; email: deposit@ccdc.cam.ac.uk or www.ccdc.cam.ac.uk/retrieving.html). Supplementary data associated with this article can be found, in the online version, at doi:10.1016/j.jorganchem.2005.06.003.

References

[1] (a) A. Müller, E. Diemann, R. Jostes, H. Bögge, Angew. Chem. Int. Ed. 20 (1981) 934;
(b) A. Müller, H. Bögge, U. Schimanski, M. Penk, K. Nieradzik, M. Dartmann, E. Krickemeyer, J. Schimanski, C. Römer, M. Römer, H. Dornfeld, U. Wienböker, W. Hellmann, Monatsh. Chem. 120 (1989) 367.

[2] (a) S. Sarkar, S.B.S. Mishra, Coord. Chem. Rev. 59 (1984) 239;
(b) M.A. Ansari, J.A. Ibers, Coord. Chem. Rev. 100 (1990) 223.

[3] (a) Y. Jeannin, F. Sécheresse, S. Bernés, F. Robert, Inorg. Chim. Acta 198–200 (1992) 493;
(b) J.R. Nicholson, A.C. Flood, C.D. Garner, W. Clegg, J. Chem. Soc., Chem. Commun. (1983) 1179.

[4] (a) E.I. Stiefel, D. Coucouvanis, W.E. Newton, Molybdenum enzymes, cofactors and model systems; ACS Symp. Ser. 535, Am. Chem. Soc., Washington, DC, 1993;
(b) E.I. Stiefel, K. Matsumoto, Transition metal sulfur chemistry, biological and industrial significance, Acs. Symp. Ser. 653, Am. Chem. Soc., Washington, DC, 1996.

[5] (a) X.T. Wu, P.C. Chen, S.W. Du, N.Y. Zhu, J.X. Lu, J. Cluster Sci. 5 (1994) 265;
(b) D.X. Wu, M.C. Hong, R. Cao, H.Q. Liu, Inorg. Chem. 35 (1996) 1080;
(c) W.J. Zhang, A. Behrens, J. Gätjens, M. Ebel, X.T. Wu, D. Rehder, Inorg. Chem. 43 (2004) 3020.

[6] (a) T. Shibahara, H. Akashi, H. Kuroya, J. Am. Chem. Soc. 110 (1988) 3313;
(b) S. Ogo, T. Suzuki, Y. Ozawa, K. Isobe, Inorg. Chem. 35 (1996) 6093.

[7] (a) C.K. Chan, C.X. Guo, R.J. Wang, T.C.W. Mak, C.M. Che, J. Chem. Soc., Dalton Trans. (1995) 753;
(b) C.M. Che, B.H. Xia, J.S. Huang, C.K. Chan, Z.Y. Zhou, K.K. Cheung, Chem. Eur. J. 7 (2001) 3998.

[8] (a) J.G. Li, X.Q. Xin, Z.Y. Zhou, K.B. Yu, J. Chem. Soc., Chem. Commun. (1990) 250;
(b) J.P. Lang, X.Q. Xin, J. Solid State Chem. 108 (1994) 118;
(c) J.P. Lang, K. Tatsumi, Inorg. Chem. 37 (1998) 6308;
(d) H.W. Hou, H.G. Zheng, G.A. How, Y.F. Fan, M.K.M. Low, Z. Yu, W.L. Wang, X.Q. Xin, W. Ji, W.T. Wong, J. Chem. Soc., Dalton Trans. (1999) 2953;
(e) H. Yu, Q.F. Xu, Z.R. Sun, S.J. Ji, J.X. Chen, Q. Liu, J.P. Lang, K. Tatsumi, Chem. Commun. (2001) 2614;
(f) J.P. Lang, Q.F. Xu, R.X. Yuan, B.F. Abrahams, Angew. Chem. Int. Ed. 43 (2004) 4741.

[9] (a) J.P. Lang, H. Kawaguchi, S. Ohnishi, K. Tatsumi, Chem. Commun. (1997) 405;
(b) J.P. Lang, K. Tatsumi, Inorg. Chem. 37 (1998) 160;
(c) J.P. Lang, H. Kawaguchi, S. Ohnishi, K. Tatsumi, Inorg. Chim. Acta 283 (1998) 136;
(d) J.P. Lang, K. Tatsumi, J. Organomet. Chem. 579 (1999) 332–337;
(e) J.P. Lang, H. Kawaguchi, K. Tatsumi, Chem. Commun. (1999) 2315;
(f) J.P. Lang, Q.F. Xu, Z.N. Chen, B.F. Abrahams, J. Am. Chem. Soc. 125 (2003) 12682;
(g) J.P. Lang, Q.F. Xu, W. Ji, H.I. Elim, K. Tatsumi, Eur. J. Inorg. Chem. (2004) 86;
(h) J.P. Lang, S.J. Ji, Q.F. Xu, Q. Shen, K. Tatsumi, Coord. Chem. Rev. 241 (2003) 47.

[10] (a) G.N. George, I.J. Pickering, E.Y. Yu, R.C. Prince, S.A. Bursakov, O.Y. Gavel, I. Moura, J.J.G. Moura, J. Am. Chem. Soc. 122 (2000) 8321;
(b) E.K. Quagraine, R.S. Reid, J. Inorg. Biochem. 85 (2001) 53.

[11] (a) S. Shi, W. Ji, S.H. Tang, J.P. Lang, X.Q. Xin, J. Am. Chem. Soc. 116 (1994) 3615;
(b) S. Shi, W. Ji, J.P. Lang, X.Q. Xin, J. Phys. Chem. 98 (1994) 3570;
(c) S. Shi, W. Ji, W. Xie, S.H. Tang, H.C. Zeng, J.P. Lang, X.Q. Xin, Mater. Chem. Phys. 39 (1995) 298;
(d) H.G. Zheng, W. Ji, M.L.K. Low, G. Sakane, T. Shibahara, X.Q. Xin, J. Chem. Soc., Dalton Trans. (1997) 2375;
(e) S. Shi, in: D.M. Roundhill, J.P. FacklerJr. (Eds.), Optoelectronic Properties of Inorganic Compounds, Plenum Press, New York, 1998, pp. 55–105;
(f) C. Zhang, Y.L. Song, B.M. Fung, Z.L. Xue, X.Q. Xin, Chem. Commun. (2001) 843;
(g) X.R. Zhu, R.M. Niu, Z.R. Sun, H.P. Zeng, Z.G. Wang, J.P. Lang, Chem. Phys. Lett. 372 (2003) 524;
(h) X.R. Zhu, Z.R. Sun, R.M. Niu, H.P. Zeng, Z.G. Wang, J.P. Lang, Z.Z. Xu, R.X. Li, J. Appl. Phys. 94 (2003) 4772.

[12] (a) F. Sécheresse, F. Robert, S. Marzak, Inorg. Chim. Acta 182 (1991) 221;
(b) S. Bernés, F. Sécheresse, Y. Jeannin, Inorg. Chim. Acta 194 (1992) 105.

[13] H. Kawaguchi, K. Tatsumi, J. Am. Chem. Soc. 117 (1995) 3885.

[14] C. Zhang, Y.L. Song, F.E. Kuhn, Y. Xu, X.Q. Xin, H.K. Fun, W.A. Herrmann, Eur. J. Inorg. Chem. (2002) 55.

[15] K. Nilsson, A. Oskarsson, Acta Chem. Scand. 36 (1982) 605.

[16] A. Müller, H. Bögge, U. Schimanski, Inorg. Chim. Acta 69 (1983) 5.

[17] Z.R. Chen, H.W. Hou, X.Q. Xin, K.B. Yu, S. Shi, J. Phys. Chem. 99 (1995) 8717.

[18] A.H. Levin, R.J. Michl, P. Ganis, U. Lepore, J. Chem. Soc., Chem. Commun. (1972) 661.

[19] G.M. Sheldrick, SHELXS-97, Program for the Solution of Crystal Structure, University of Goettingen, Germany, 1997.

[20] P.T. Beurskens, G. Admiraal, G. Beurskens, W.P. Bosman, R. de Gelder, R. Israel, J.M.M. Smits, DIRDIF99, The DIRDIF-99 Program System, Technical Report of the Crystallography Laboratory, University of Nijmegen, The Netherlands, 1999.

[21] D.T. Cromer, J.T. WaberInternational Tables for X-ray Crystallography, vol. IV, The Kynoch Press, Birmingham, England, 1974, Table 2.2 A.

[22] J.A. Ibers, W.C. Hamilton, Acta Crystallogr. 17 (1964) 781.

[23] (a) K.M. Nashold, D.P. Walter, J. Opt. Soc. Am. B 12 (1995) 1228;
(b) R.L. McLean, M.C. Sutherland, M.C. Brant, D.M. Brandelik, P.A. Fleitz, T. Pottenger, Opt. Lett. 18 (1993) 858.